NUCLEAR FUSION DEFECTIVE1 Encodes the Arabidopsis RPL21M Protein and Is Required for Karyogamy during Female Gametophyte Development and Fertilization[1]

Michael F. Portereiko, Linda Sandaklie-Nikolova, Alan Lloyd, Chad A. Dever, Denichiro Otsuga, and Gary N. Drews*

Department of Biology, University of Utah, Salt Lake City, Utah 84112–0840

Karyogamy, or nuclear fusion, is essential for sexual reproduction. In angiosperms, karyogamy occurs three times: twice during double fertilization of the egg cell and the central cell and once during female gametophyte development when the two polar nuclei fuse to form the diploid central cell nucleus. The molecular mechanisms controlling karyogamy are poorly understood. We have identified nine female gametophyte mutants in Arabidopsis (*Arabidopsis thaliana*), *nuclear fusion defective1* (*nfd1*) to *nfd9*, that are defective in fusion of the polar nuclei. In the *nfd1* to *nfd6* mutants, failure of fusion of the polar nuclei is the only defect detected during megagametogenesis. *nfd1* is also affected in karyogamy during double fertilization. Using transmission electron microscopy, we showed that *nfd1* nuclei fail to undergo fusion of the outer nuclear membranes. *nfd1* contains a T-DNA insertion in *RPL21M* that is predicted to encode the mitochondrial 50S ribosomal subunit L21, and a wild-type copy of this gene rescues the mutant phenotype. Consistent with the predicted function of this gene, an NFD1-green fluorescent protein fusion protein localizes to mitochondria and the *NFD1/RPL21M* gene is expressed throughout the plant. The *nfd3*, *nfd4*, *nfd5*, and *nfd6* mutants also contain T-DNA insertions in genes predicted to encode proteins that localize to mitochondria, suggesting a role for this organelle in nuclear fusion.

Karyogamy is the process by which two nuclei fuse to produce a single nucleus. Karyogamy is required during mating in a wide variety of organisms, for example, during fusion of egg and sperm in plants and animals (van Went and Willemse, 1984), and during mating of a and α cells in yeast (*Saccharomyces cerevisiae*; Rose, 1996).

Karyogamy occurs three times during the angiosperm life cycle. Two of these karyogamy events occur during double fertilization. Upon entry of the pollen tube into the ovule, two sperm cells are released into the female gametophyte. One sperm fertilizes the egg cell and the second fertilizes the central cell, giving rise to the seed's embryo and endosperm, respectively (Maheshwari and Johri, 1950; Weterings and Russell, 2004).

The third karyogamy event takes place during female gametophyte development. As shown in Figure 1, late during megagametogenesis, two nuclei, the polar nuclei, migrate toward the female gametophyte's center and fuse. In Arabidopsis (*Arabidopsis thaliana*) and other species, fusion is completed prior to fertilization, whereas in maize (*Zea mays*) and other species, the polar nuclei only partially fuse before fertilization (Willemse and van Went, 1984; Huang and Russell, 1992). Karyogamy during female gametophyte development is important because it produces the secondary nucleus, which subsequently fuses with one of the sperm nuclei and gives rise to the triploid endosperm.

Little is known about the molecular processes controlling and mediating nuclear fusion in plants, and mutants affected in karyogamy during fertilization have not been reported. However, a number of mutants affected in fusion of the polar nuclei during female gametophyte development have been identified, including *magatama1* (*maa1*) and *maa3* (Shimizu and Okada, 2000), *gametophytic factor2* (*gfa2*; Christensen et al., 2002), *Glc-6-P/phosphate translocator1* (*gpt1*; Niewiadomski et al., 2005), and EMBRYO SAC DEVELOPMENT ARREST24 (EDA24) to EDA41 (Pagnussat et al., 2005). GFA2 is a J-domain-containing protein similar to yeast Mdj1p, which functions as a chaperone in the mitochondrion (Christensen et al., 2002). GPT1 is required for fatty acid biosynthesis (Niewiadomski et al., 2005). The roles of GFA2 and GPT1 in nuclear fusion are unknown. The genes affected in the *maa1* and *maa3* mutants have not been identified, and the genes affected in the EDA24 to EDA41 mutants have not been analyzed at the molecular level; thus, the molecular

[1] This work was supported in part by Ceres, Inc. (grant to G.N.D.) and the U.S. Department of Agriculture (Cooperative State Research, Education and Extension Service fellowship no. 2004–35304–14931 to M.F.P.).

* Corresponding author; e-mail drews@bioscience.utah.edu; fax 801–581–4668.

The author responsible for distribution of materials integral to the findings presented in this article in accordance with the policy described in the Instructions for Authors (www.plantphysiol.org) is: Gary N. Drews (drews@bioscience.utah.edu).

Article, publication date, and citation information can be found at www.plantphysiol.org/cgi/doi/10.1104/pp.106.079319.

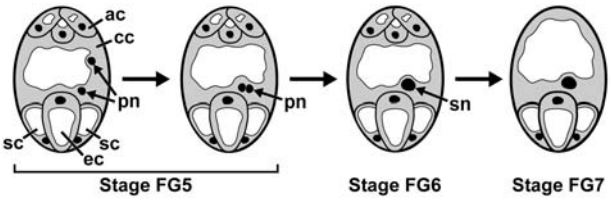

Figure 1. Karyogamy during female gametophyte development in Arabidopsis. Female gametophyte developmental stages: The megaspore (stage FG1; not shown) undergoes three rounds of mitosis and cellularization and results in a seven-celled, eight-nucleate female gametophyte (stage FG5). The central cell inherits two nuclei (polar nuclei), which migrate toward the female gametophyte's center and fuse to form the secondary nucleus (stage FG6). Finally, the antipodal cells degenerate, producing a mature female gametophyte (stage FG7). ac, Antipodal cells; cc, central cell; ec, egg cell; pn, polar nuclei; sc, synergid cell; sn, secondary nucleus. In these images, nuclei are black, cytoplasm is gray, and vacuoles are white.

basis of the nuclear fusion defects in these mutants is not understood.

To further the molecular analysis of karyogamy in angiosperms, we have identified and analyzed a battery of mutants defective in fusion of the polar nuclei during female gametophyte development. One of these mutants, *nuclear fusion defective1* (*nfd1*), is also affected in karyogamy during fertilization. Using transmission electron microscopy (TEM), we show that *nfd1* is affected in fusion of the outer nuclear membranes. The *NFD1* gene encodes mitochondrial ribosomal protein L21, suggesting a role for this organelle in karyogamy.

RESULTS

Identification of Nine Mutants Affected in Karyogamy during Female Gametophyte Development

During the angiosperm life cycle, karyogamy occurs first during female gametophyte development when the polar nuclei fuse (Fig. 1) and later during fertilization when the sperm nuclei fuse with the female gametophyte's egg and central cell nuclei. Therefore, mutations affecting karyogamy should affect the female gametophyte and, as a consequence, should result in segregation distortion and reduced seed set (Drews and Yadegari, 2002). Using these criteria, we previously identified a large collection of female gametophyte mutants (Yadegari and Drews, 2004). Within this mutant collection were nine mutants with defects in fusion of the polar nuclei. We have named these mutants *nfd1* to *nfd9.*

Analysis by confocal laser-scanning microscopy (CLSM) of the female gametophytes from the *nfd1* to *nfd9* mutants is summarized in Table I. In all nine mutants, the polar nuclei migrated properly but failed to fuse, indicating that nuclear congression is not affected (Fig. 2, A and B). In six of the mutants (*nfd1–nfd6*), failure of fusion of the polar nuclei was the only defect observed during female gametophyte development. In contrast, in the other three mutants (*nfd7–nfd9*), additional defects were observed (Table I). Segregation analysis of the *nfd1* to *nfd9* mutants is summarized in Table II and indicates that mutant alleles affect both the female and male gametophytes. The remainder of this article is focused on the *nfd1* to *nfd6* mutants that are affected specifically in fusion of the polar nuclei during female gametophyte development.

nfd1 Affects Karyogamy during Fertilization

We next asked whether the *nfd1* to *nfd6* mutants are also affected in karyogamy during fertilization. The fertilization process in Arabidopsis wild type has been described by Faure et al. (2002). Pollen tubes enter the female gametophyte by growing into one of the synergid cells. This synergid cell undergoes cell death just before or upon pollen tube entry. The pollen tube then releases its contents into the degenerating synergid cell, and the sperm cells migrate to and fuse with the egg cell and central cell (plasmogamy). Plasmogamy triggers changes in the polarity and morphology of the egg cell (Fig. 2C). Following plasmogamy, the sperm nuclei can be observed transiently within the egg cell and the central cell. The sperm nuclei then fuse with the egg and central cell nuclei (karyogamy) to produce the diploid zygote and triploid endosperm nuclei, respectively. One to 2 h after karyogamy, the endosperm

Table I. *Summary of CLSM analysis of the nfd1 to nfd9 mutants*

FG, Female gametophyte; PN, polar nuclei; WT, wild type.

Genotype	FG Phenotype						
	No FG	One to Four Nuclei Uncellularized	Eight Nuclei Uncellularized	Persistent Antipodals	Unfused PN	WT	*n*
nfd1/NFD1					42%	58%	198
nfd2/NFD2					40%	60%	118
nfd3/NFD3					48%	52%	162
nfd4/NFD4					36%	64%	133
nfd5/NFD5					29%	71%	187
nfd6/NFD6					25%	75%	154
nfd7/NFD7			5%	6%	28%	61%	139
nfd8/NFD8			29%		8%	63%	177
nfd9/NFD9	7%	18%			26%	49%	100

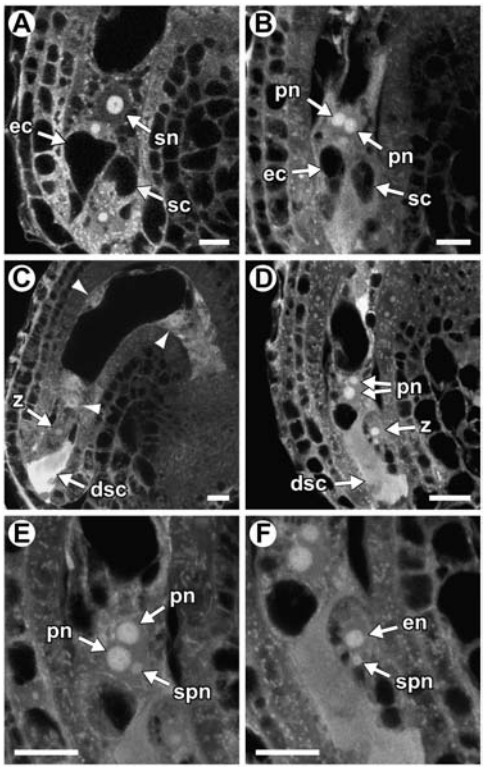

Figure 2. CLSM analysis of wild-type and *nfd1* female gametophytes. A and B, Wild type (A) and *nfd1* (B) female gametophytes at the terminal developmental stage (stage FG7). In wild type (A), the polar nuclei have fused to form the diploid secondary nucleus. A wild-type egg cell (A) contains a single, large vacuole and has a nucleus at the chalazal pole. In *nfd1* (B), the polar nuclei remain unfused. C to F, Wild-type (C) and *nfd1* (D–F) seeds at 18 h after pollination. The wild-type seed (C) contains a degenerating synergid cell, a zygote, and four endosperm nuclei (arrowheads; only three endosperm nuclei are in this focal plane). A wild-type zygote (C) is relatively round (in comparison to the egg cell), contains many small vacuoles, and has a centrally located nucleus. *nfd1* (D) contains a degenerated synergid cell, a zygote, two unfused polar nuclei, and no endosperm nuclei. E and F, Magnified images from the same ovule as in D. The image in E is of a different focal plane than that in D. The image in F is of the same focal plane as that in D. In E, the polar nuclei and the sperm nucleus are visible within the central cell. In F, the egg cell nucleus and the sperm nucleus are visible within the zygote. In these images, cytoplasm is gray, vacuoles are black, and nucleoli are white. dsc, Degenerating synergid cell; ec, egg cell; en, egg cell nucleus; pn, polar nucleus; sc, synergid cell; sn, secondary nucleus; spn, sperm nucleus; z, zygote. Scale bars = 10 μm.

nucleus divides once to produce a binucleate endosperm. By 18 h after pollination, the endosperm consists of four to eight nuclei and the zygote remains undivided (Fig. 2C; Faure et al., 2002).

To determine whether the *nfd* mutants are affected in karyogamy during fertilization, we pollinated pistils from heterozygous mutants with wild-type pollen and analyzed the ovules at 18 h after pollination. In *nfd1*, synergid cell degeneration occurred normally and egg cell morphology was altered as it is following plasmogamy in the wild type (Fig. 2, D and F). These features indicate that pollen tube guidance, synergid cell death, pollen tube entry, release of pollen tube contents, sperm cell migration, and plasmogamy occur normally in *nfd1* female gametophytes. However, in contrast to wild-type female gametophytes at this time point, sperm nuclei were persistent within both the egg cell (Fig. 2F) and the central cell (Fig. 2E), and the endosperm was undivided (Fig. 2D). These data suggest that *nfd1* female gametophytes are defective in karyogamy during fertilization. The other five mutants (*nfd2–nfd6*) exhibited defects before sperm release, precluding observation of karyogamy during fertilization.

The unfused sperm nuclei present in *nfd1* female gametophytes could be due to either a defect in karyogamy during fertilization or a delay in the fertilization process. To distinguish between these possibilities, we analyzed *nfd1* female gametophytes at 24 and 48 h after pollination. In the wild type, the majority of seeds have an undivided zygote and eight endosperm nuclei at 24 h after pollination (Boisnard-Lorig et al., 2001), and a globular-stage embryo and >50 endosperm nuclei at 48 h after pollination (Boisnard-Lorig et al., 2001). In *nfd1* at 24 h after pollination, sperm nuclei were still observed within the egg and central cells (data not shown). At 48 h after pollination, *nfd1* embryo sacs were undergoing senescence, which is an indication that fertilization had not been completed. The senescence obscured observation of persistent sperm nuclei; however, mutant female gametophytes did not contain developing embryos or endosperm (data not shown), as would be the case if the *nfd1* defect were due to developmental delay. Together, these data indicate that *nfd1* female gametophytes have a defect in karyogamy during fertilization in both the egg cell and the central cell.

nfd1 Affects the First Step of Nuclear Fusion

To determine which step of karyogamy is affected in *nfd1* female gametophytes, we used TEM to analyze

Table II. *Transmission of the nfd1 to nfd9 mutations*

Parental Genotype		No. Progeny	
Male	Female	*NFD/NFD*	*nfd/NFD*
NFD1/NFD1	*nfd1/NFD1*	556	116
nfd1/NFD1	*NFD1/NFD1*	420	93
NFD2/NFD2	*nfd2/NFD2*	927	46
nfd2/NFD2	*NFD2/NFD2*	699	0
NFD3/NFD3	*nfd3/NFD3*	667	173
nfd3/NFD3	*NFD3/NFD3*	194	6
NFD4/NFD4	*nfd4/NFD4*	254	84
nfd4/NFD4	*NFD4/NFD4*	356	185
NFD5/NFD5	*nfd5/NFD5*	404	77
nfd5/NFD5	*NFD5/NFD5*	289	15
NFD6/NFD6	*nfd6/NFD6*	311	99
nfd6/NFD6	*NFD6/NFD6*	375	23
NFD7/NFD7	*nfd7/NFD7*	267	13
nfd7/NFD7	*NFD7/NFD7*	251	60
NFD8/NFD8	*nfd8/NFD8*	291	3
nfd8/NFD8	*NFD8/NFD8*	286	0
NFD9/NFD9	*nfd9/NFD9*	139	26
nfd9/NFD9	*NFD9/NFD9*	137	5

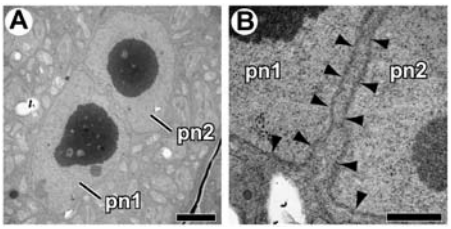

Figure 3. TEM analysis of the unfused polar nuclei in *nfd1* female gametophytes. A and B, Electron micrographs of the central cell of female gametophytes at the terminal developmental stage (stage FG7). The nucleoli (dark gray) are surrounded by a nucleoplasm (light gray) and a nuclear envelope (arrowheads). Scale bars = 3 μm (A) and 1 μm (B). pn, Polar nucleus.

the unfused polar nuclei in this mutant. The nuclear fusion process has been characterized using TEM in a wide variety of plant species (Jensen, 1964; van Went, 1970; Schulz and Jensen, 1973; Maze and Lin, 1975; Folsom and Peterson, 1984; Sumner and van Caeseele, 1990; Faure et al., 1993). During both megagametogenesis and fertilization, karyogamy occurs between intact nuclei and begins with contact of the endoplasmic reticulum (ER) membranes that are continuous with the outer nuclear membranes of the two nuclei. Fusion of the membranes results in outer nuclear membranes that are continuous. Finally, the inner nuclear membranes come into contact and merge, resulting in a mixing of the nucleoplasm and chromosomes.

We analyzed the unfused polar nuclei in *nfd1* female gametophytes at the terminal developmental stage (stage FG7). Consistent with our CLSM analysis, the two polar nuclei were adjacent to each other (Fig. 3A), indicating that there were no defects in nuclear congression. The nuclear envelopes were spherical except at their apposing faces, where the nuclear membranes were relatively flat (Fig. 3). The outer nuclear membranes were not in contact with each other. A gap ranging in size from approximately 50 to 600 nm existed between the two nuclei along the entire length of the interface (Fig. 3B). These observations suggest that *nfd1* female gametophytes are defective specifically in the initial step of nuclear fusion, fusion of the outer nuclear membranes.

nfd1 Affects Male Gametophyte Development

As shown in Table II, transmission of the *nfd1* mutation is also reduced through the male gametophyte. To determine whether *nfd1* affects male gametophyte development or a subsequent step (e.g. nuclear fusion), we analyzed mature pollen using CLSM. As shown in Figure 4B, anthers from *nfd1/NFD1* contained numerous collapsed pollen grains. On average (n = 4 plants), 43% of pollen grains from *nfd1/NFD1* plants were collapsed (n = 400). By contrast, wild-type anthers contained only 2% collapsed pollen grains (n = 200). These data indicate that the *nfd1* mutation affects male gametophyte development.

NFD1 Encodes the Mitochondrial 50S Ribosomal Subunit L21

The *nfd1* mutant was identified in a screen of T-DNA-mutagenized lines. To identify the gene affected in the *nfd1* mutant, we determined the T-DNA insertion site using thermal asymmetric interlaced (TAIL)-PCR (Liu et al., 1995). The T-DNA is inserted into gene At4g30925 in *nfd1*. To determine whether the female gametophyte defect is due to disruption of At4g30925, we introduced a wild-type copy of this gene into the *nfd1* mutant. We identified T1 plants heterozygous for *nfd1* and hemizygous for the rescue construct and crossed these as females with wild-type males. In the F_1 generation, *nfd1/NFD1* and *NFD1/NFD1* progeny were present in a ratio of approximately 1:2. In addition, we generated plants homozygous for the *nfd1* allele and homozygous for the rescue construct; these plants had full seed set. These data indicate that disruption of the At4g30925 gene is responsible for the female gametophyte defect in *nfd1* mutants.

At4g30925 corresponds to *RPL21M*, which is predicted to encode the mitochondrial 50S ribosomal subunit L21. As shown in Figure 5, this gene spans 1,819 bp, contains an open reading frame of 813 bp, and encodes a protein of 270 amino acids. The predicted protein contains a region with high similarity (36% identical and 56% similar) to the L21p protein of *Escherichia coli* (Fig. 5B). Analysis of this protein by the TargetP algorithm (Emanuelsson et al., 2000) predicts mitochondrial localization and NH_2-terminal peptide cleavage after amino acid 68. Consistent with these predictions, RPL21M has an overrepresentation of Arg, Ala, and Ser (23/68) and an underrepresentation of Asp and Glu residues (3/68; Fig. 5B) in the NH_2-terminus of the protein, which is typical of proteins targeted to mitochondria (Gavel et al., 1988; Roise, 1997). The gene family containing *RPL21M* includes only one other gene within the Arabidopsis genome, At1g35680, which is predicted to encode the plastid 50S ribosomal L21 subunit based on the presence of chloroplast-sorting motifs (TargetP) and similarity to the spinach (*Spinacia oleracea*) plastid *RPL21* gene (Lagrange et al., 1993).

As shown in Figure 5A, the left and right borders of the T-DNA in *nfd1* are inserted into the first and

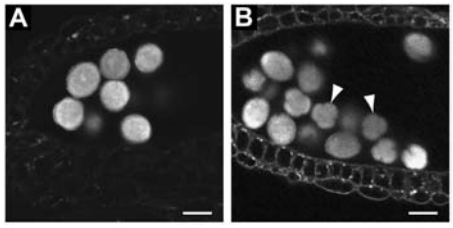

Figure 4. CLSM analysis of pollen from wild type and *nfd1/NFD1*. A, Pollen from wild-type anthers. The pollen grains are round. B, Pollen from *nfd1/NFD1* anthers. Both round and collapsed pollen grains are present. Arrowheads indicate two of the collapsed pollen grains in this image. Scale bars = 20 μm (A and B).

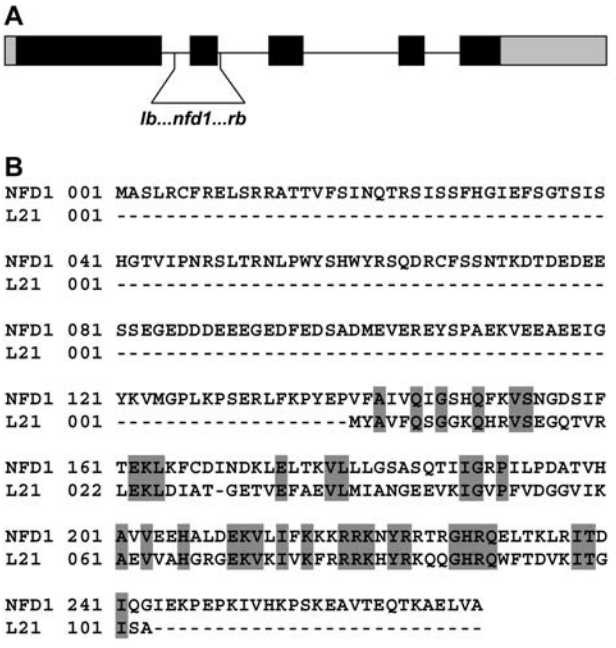

Figure 5. *NFD1* gene structure and protein alignment. A, *NFD1* gene structure. Black boxes represent coding sequence, gray boxes represent UTRs, and the horizontal line represents intron sequence. The vertical lines represent the T-DNA insertion sites in *nfd1*. B, Comparison of the amino acid sequence between NFD1 and the L21p protein in *E. coli*. Conserved amino acids are in gray.

second introns of At4g30925, respectively, and are associated with a 138-bp deletion that removes the entire second exon, which encodes amino acids 146 to 173. This observation suggests that *nfd1* is a null allele. However, we were not able to confirm this prediction because we were unable to obtain a line homozygous for the *nfd1* mutation and, thus, were not able to analyze *NFD1* expression in *nfd1* mutants.

NFD1 Is Expressed throughout the Plant

To determine where *NFD1* is expressed within the plant, we performed reverse transcription (RT)-PCR with RNA from various organs. As shown in Figure 6, a signal was detected in all tissues tested, including roots, stems, leaves, young flowers, mature-stage pistils, and siliques (Fig. 6). These data indicate that *NFD1* is expressed throughout the plant.

To determine the subcellular localization of NFD1, we analyzed transgenic Arabidopsis plants containing a protein fusion construct in which the *NFD1* promoter and the entire *NFD1* open reading frame were fused to a green fluorescent protein (GFP) coding sequence (*NFD1-GFP*). In transgenic plants containing the *NFD1-GFP* construct, GFP was detected in multiple small intracellular compartments (Fig. 7A). This pattern colocalized with MitoTracker, a mitochondrion-specific dye (Fig. 7, B and C). *NFD1-GFP* expression was detected in all organs examined, including roots, leaves, embryos, and ovules (data not shown). These data suggest that NFD1 protein localizes to mitochondria, consistent with its predicted function as the mitochondrial 50S ribosomal subunit L21.

Identification of Genes Disrupted in the *nfd2* to *nfd6* Mutants

We used TAIL-PCR to identify the T-DNA insertion sites in the *nfd2* to *nfd6* mutants (Table III). We then performed linkage studies and showed that all of the identified T-DNAs were linked to the mutant phenotypes. Four of the genes (*NFD3*, *NFD4*, *NFD5*, and *NFD6*) encode proteins predicted to localize to the mitochondrion (Table III). *NFD3* is predicted to encode the 30S ribosomal subunit S11, and *NFD5* and *NFD6* do not have significant sequence similarity to any known proteins. *NFD4* is predicted to encode a protein that is nodulin-like. *NFD2* is predicted to encode a protein that contains a ribonuclease III domain and to localize to the endomembrane system.

DISCUSSION

Little is known about karyogamy at the molecular level. Genetic and biochemical studies of karyogamy have been performed in yeast, which undergoes nuclear fusion by a process similar to that in plants (Ng and Walter, 1996; Rose, 1996). These studies have identified six proteins required for nuclear fusion, including Kar5p, Kar2p, Kar8p/Jem1p, Kar7p/Sec71p, Sec63p, and Sec72p (Ng and Walter, 1996; Rose, 1996). Kar5p is a novel integral ER-nuclear envelope membrane protein that localizes near the spindle pole body (Beh et al., 1997; Brizzio et al., 1999). Kar2p is a homolog of mammalian BiP that belongs to the Hsp70 family and localizes to the lumen of the ER. Kar8p/Jem1p is an ER-resident DnaJ protein. Kar7p/Sec71p, Sec63p, and Sec72p are components of the translocon, a complex embedded in the ER membrane responsible for protein translocation into the ER (Brizzio et al., 1999); genetic and biochemical studies have shown that the role of these proteins in the translocon is distinct from their function in membrane fusion (Ng and Walter, 1996). The roles of the translocon-associated proteins and the other three proteins in nuclear fusion remain unclear.

We have identified and analyzed a battery of mutants defective in fusion of the polar nuclei during female gametophyte development. With six of these mutants (*nfd1–nfd6*), failure of fusion of the polar

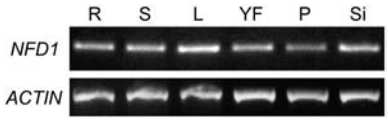

Figure 6. RT-PCR analysis of *NFD1* expression. Shown is RT-PCR analysis of *NFD1* in roots (R), inflorescence stems (S), leaves (L), young flowers (YF), pistils (P), and siliques (Si). Expression of *ACTIN* was used as a control.

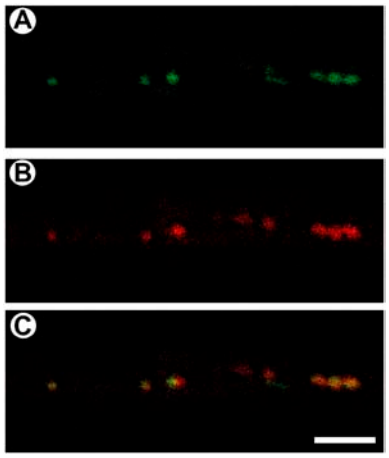

Figure 7. NFD1-GFP localization. Shown are CLSM images of a MitoTracker-stained root from a transgenic plant expressing *NFD1-GFP*. A, GFP fluorescence. B, MitoTracker red fluorescence. C, Merge of A and B. Scale bar = 5 μm.

nuclei is the only defect detected during megagametogenesis (Table I). One of these mutants, *nfd1*, is also affected in karyogamy during fertilization (Fig. 2, D–F). Using TEM, we showed that *nfd1* nuclei fail to undergo fusion of the outer nuclear membranes (Fig. 3), which could result from a defect in either recognition between the outer membranes of the two nuclei or in initiation of the membrane fusion process.

NFD1 encodes mitochondrial protein L21, which is a component of the ribosome's large (50S) subunit. In *E. coli*, L21 binds to 23S ribosomal RNA (Alexander and Cooperman, 1998; Vladimirov et al., 2000), which plays a direct role in protein synthesis (Samaha et al., 1995). Thus, *nfd1* mutants are likely to be affected in protein synthesis within the mitochondrion. The genome of the Arabidopsis mitochrondrion contains 33 protein-coding genes that encode proteins involved in electron transport, oxidative phosphorylation, heme and cytochrome assembly, and ribosome structure (Unseld et al., 1997). These processes are likely to be impaired in *nfd1* female gametophytes. *NFD1* encodes the only mitochondrially targeted L21 ribosomal subunit in the Arabidopsis genome; therefore, it is expected to function throughout the plant. Consistent with this prediction, *NFD1* is expressed throughout the plant (Fig. 6), NFD1-GFP localizes to mitochondria (Fig. 7), and the *nfd1* mutation exhibits reduced transmission through both the female and the male gametophytes (Table II).

At this time, it is unclear why *nfd1* mutants have a nuclear fusion defect. One possibility is that the karyogamy defect is a secondary consequence of a defect in electron transport and ATP production. However, many cellular and physiological processes occur normally in *nfd1* female gametophytes, including mitosis, vacuole formation, cell wall formation, cell death, pollen tube guidance, control of pollen tube growth cessation and release of pollen tube content, plasmogamy, and sperm migration. These observations suggest that *nfd1* female gametophytes are not completely energy deficient, possibly due to inheritance and persistence of wild-type mitochondria from the diploid megaspore mother cell or transfer of ATP from the surrounding sporophytic cells. However, we cannot rule out the possibility that *nfd1* female gametophytes have reduced energy stores and that initiation of nuclear membrane fusion is more sensitive than other processes to this reduction.

An alternative possibility is that the *nfd1* mutation affects karyogamy for reasons other than energy production. In this regard, *MRPL49*, the homolog of *NFD1* in yeast, appears to be required for phosphatidylcholine (PC) biosynthesis (Hancock et al., 2006). At this time, it is unclear whether *mrpl49* mutants are affected in PC biosynthesis directly or indirectly through an effect on mitochondria. PC constitutes >50% of the phospholipids of the nuclear membrane in plants (Philipp et al., 1976). These observations suggest that the *nfd1* mutation may alter the phospholipid composition of the nuclear membrane. Changes in phospholipid composition have been shown to affect vesicle fusion (Duzgunes et al., 1981) and nuclear membrane growth (Santos-Rosa et al., 2005). Thus, *nfd1* may affect nuclear fusion by altering phospholipid content within the nuclear membrane.

A number of other nuclear fusion mutants have defects in genes encoding mitochondrial proteins. These mutants include *nfd3*, *nfd4*, *nfd5*, and *nfd6* (Table III)

Table III. *T-DNA insertion sites in the nfd1 to nfd6 mutants*

ND, Not determined.

Mutant	Gene ID[a]	Predicted Identity	Predicted Localization[b]	Gene Insertion Site	Left-Border Position	Right-Border Position
nfd1	At4g30925	50S ribosomal subunit L21	Mitochondria	Intron 1	AGI 15051022	AGI 15051159
nfd2	At1g24450	Ribonuclease III domain	Secretory pathway	Promoter	AGI 8664098	ND
nfd3	At1g31817	30S ribosomal subunit S11	Mitochondria	Intron 1	AGI 11416137	ND
nfd4	At1g31470	Nodulin related	Mitochondria	Exon 2	AGI 11263904[c]	–
					AGI 11263882[c]	–
nfd5	At1g19520	None	Mitochondria	Exon 1	AGI 6759897	AGI 6759964
nfd6	At2g20585	None	Chloroplast or mitochondria	Exon 1	AGI 8872213	AGI 8872234

[a]MIPS database. [b]Based on TargetP. [c]T-DNA associated with *nfd4* has two left borders.

identified in this study, as well as the previously reported mutants *gfa2* (Christensen et al., 2002) and EDA28 and EDA35 (Pagnussat et al., 2005). Analysis of other nuclear fusion mutants as well as mitochondrial mutants in Arabidopsis and yeast should help to clarify the possible role of the mitochondrion in nuclear fusion in these two organisms.

MATERIALS AND METHODS

Plant Materials

The isolate numbers for the mutant lines described in this article are as follows: *nfd1*, G430 (*fem55*); *nfd2*, G683 (*fem56*); *nfd3*, LE156 (*fem60*); *nfd4*, DO2566 (*fem113*); *nfd5*, DO1861 (*fem118*); *nfd6*, DO1867 (*fem119*); *nfd7*, DO43; *nfd8*, DO1463; and *nfd9*, DO2399.

Growth Conditions

Seeds were sterilized in a solution of 50% commercial bleach and 0.1% Tween 20 and germinated on plates containing 0.5× Murashige and Skoog salts (M–9274; Sigma), 0.05% MES, 0.5% Suc, and 0.8% phytagar (Life Technologies). Ten-day-old seedlings were transferred to Scott's Redi-Earth and grown under 24-h illumination.

Plant Transformation

T-DNA constructs were introduced into Agrobacterium strain LBA4404 by electroporation. Arabidopsis (*Arabidopsis thaliana* ecotype Columbia) plants were transformed using a modified floral-dip procedure (Clough and Bent, 1998). Transformed progeny were selected by germinating surface-sterilized T1 seeds on growth medium containing antibiotics. Resistant seedlings were transplanted to soil after 10 d of growth.

Genetic Analysis of Mutants

Reciprocal crosses were carried out between each heterozygous mutant and wild type as indicated in Table II. F_1 seed was collected and germinated on medium containing 50 μg/mL kanamycin. Resistant and sensitive plants were scored as heterozygous and homozygous wild type, respectively.

Confocal Analysis

CLSM analysis of ovules was performed as described previously (Christensen et al., 1997, 1998, 2002) with use of a Zeiss LSM510 microscope as a modification. For analysis of female gametophytes at the terminal developmental stage (stage FG7), we emasculated flowers from heterozygous mutant plants at stage 12c (Christensen et al., 1997), waited 24 to 40 h, and harvested the specimens for fixation. For analysis after pollination, we emasculated flowers from heterozygous mutant plants at stage 12c, waited 24 h, pollinated with wild-type pollen, waited 18 to 48 h, and harvested the siliques for fixation.

CLSM analysis of pollen grains was performed as follows. Flowers at stage 13 (Smyth et al., 1990) were harvested and placed into a fixation solution of 4% glutaraldehyde and 10 mM cacodylate in water for 2 h. The flowers were then dehydrated in an ethanol series (10%, 20%, 40%, 60%, 80%) for 10 min each followed by 95% ethanol overnight. The flowers were incubated for 20 min in a 2:1 solution of benzyl benzoate and benzyl alcohol and then placed into immersion oil where the stamens were removed. The stamens were then placed onto microscope slides in a drop of immersion oil. Microscopic analysis was performed as described for ovules.

TEM

TEM analysis was performed as described previously (Kasahara et al., 2005). Three *nfd1* female gametophytes at the terminal developmental stage were analyzed. For each gametophyte analyzed, at least five serial sections were observed to determine whether the outer nuclear envelopes were in contact.

Characterization of the T-DNA Flanking Sequences in *nfd* Mutants

We performed TAIL-PCR (Liu et al., 1995) to identify the sequences flanking the T-DNA insertions. We then performed PCR reactions using T-DNA-specific and genome-specific primers to verify the T-DNA flanking sequences. The T-DNA-specific primers used were L1 (5′-CTCAATGCAAAAGGGGAACG-3′) for the T-DNA left border and RB2 (5′-CATAACGTCGACTCCCTTAATTCTC-3′) for the T-DNA right border. For *nfd1*, primer L1 was used with gene-specific primer RPL21M-LB2 (5′-ACCGGCGGAGAAAGTGGAAGAG-3′) and primer RB2 was paired with gene-specific primer RPL21M-RP (5′-TGCCGAGCCCAATAGAAGAAC-3′). For *nfd2*, primer L1 was used with gene-specific primer At1G24450-rb (5′-AGATCCCGACGACGAAGACAAGA-3′). For *nfd3*, primer L1 was used with gene-specific primer At1G31817-rb (5′-TCCCGTGTTTGATAAGCCTGAA-3′). For *nfd4*, primer L1 was used with gene-specific primers At1g31470-lp (5′-CGAGCCTCACTGTGTTCCCTTCC-3′) and At1G31470-rp (5′-TTAACCCGTCGTCGTCCAATCTAT-3′). For *nfd5*, primer L1 was used with gene-specific primer At1G19520-lp (5′-GAGCACAGGGTCAAAAGAGAAAC-3′) and primer RB2 was used with gene-specific primer At1G19520-rp (5′-GTCAATGGCGGCACTGGAT-3′). For *nfd6*, primer L1 was used with gene-specific primer At2G20585-lp (5′-TTTTTAATCGCCACCAAGTC-3′) and primer RB was used with gene-specific primer At2G20585-rp (5′-GCGAAGCGGCCAGTAGAAGC-3′).

In *nfd1*, the T-DNA is associated with a 137-bp deletion that spans from +514 to +651 bp relative to the predicted start of transcription of gene At4g30925. In *nfd2*, only the flanking sequence adjacent to the left border of the T-DNA insertion was identified and the T-DNA insertion site is 45 bp, 5′ of the predicted transcription start site of gene At1G24450. For *nfd3*, only the flanking sequence adjacent to the left border of the T-DNA insertion was identified and the T-DNA insertion site is at +280 bp relative to the predicted transcription start site of gene At1G31817. For *nfd4*, the T-DNA insertion had two left borders and the T-DNA insertion site is associated with a 22-bp deletion in the second exon from +913 to +935 bp relative to the ATG of At1g31470. For *nfd5*, the T-DNA insertion site is associated with a 65-bp deletion that includes the first 11 bp of the 5′-untranslated region (UTR) of gene At1G19520 and an additional 54 bp of the 5′ flanking sequence. For *nfd6*, the T-DNA insertion site is associated with a 21-bp deletion in the 5′-UTR of gene At2g20585 from +33 to +55 bp relative to the predicted start of transcription.

NFD1 Gene Structure and Molecular Complementation of the *nfd1* Mutation

NFD1 gene structure is based on comparison of the genome sequence and the sequences of two previously reported cDNAs (CERES:7876 and EMBL: BT005870.1; http://mips.gsf.de/cgi-bin/proj/thal/search_gene?code=at4g30925).

Molecular complementation was performed using a 2,800-bp DNA fragment containing the *NFD1* genomic coding sequence (1,461 bp) along with 474 bp of sequence upstream of the translational start codon and 865 bp of sequence downstream of the stop codon. This DNA fragment was amplified by PCR using the primers nfd1F2 (5′-GCTGCAGCCGCTCCAACATC-3′; contains a native *Pst*I site) and nfd1R2 (5′-TTGAGTAACGCACTGAGCTTC-3′). This 2.8-kb PCR product was TOPO cloned into vector pPCR II (Invitrogen) in an orientation such that the *Pst*I sites within the vector and the PCR product were on opposite ends to make plasmid NFD1-2.8 TOPO. The *Pst*I-*Pst*I fragment within NFD1-2.8 TOPO was subcloned into pCAMBIA1300, producing plasmid NFD1-2.8-pCAMBIA. pCAMBIA1300 contains a marker gene conferring resistance to hygromycin. NFD1-2.8-pCAMBIA was introduced into Arabidopsis plants as described above and transformed plants were selected by germinating seeds on growth medium containing 15 μg/mL hygromycin. Hygromycin-resistant plants containing the *nfd1* allele were identified by PCR by using primers oligo-L1 (discussed above) and RPL21M-LB2 (discussed above).

T1 plants containing the rescue construct at a single locus were identified based upon a 3:1 ratio of hygromycin-resistant to hygromycin-sensitive plants in the T_2 generation. Plants heterozygous for the *nfd1* allele and hemizygous for the rescue construct at a single locus were crossed as females with wild-type males and the F_1 seed was germinated on growth medium containing 50 μg/mL kanamycin. We observed 53 kanamycin-resistant (scored as being

genotype *nfd1/NFD1*) and 78 kanamycin-sensitive (scored as being genotype *NFD1/NFD1*) progeny. Plants homozygous for both the *nfd1* mutation and the rescuing construct were obtained by identifying F_1s (from the double heterozygote) whose progeny was both 100% kanamycin and 100% hygromycin resistant.

NFD1-GFP Protein Localization

The *NFD1-GFP* fusion construct has GFP inserted 30 bp upstream of the stop codon of the *NFD1* gene. As a first step in cloning this gene, we generated three PCR products. An upstream fragment was amplified using primers FEM55GFPF1 (5′-CAGGTATACTTTATAACTCC-3′; includes a native *Acc*I site) and FEM55GFPR1 (5′-CTCGCCCTTGCTCACCATAACAGCTTCTTTC-GAAGG-3′; contains 18 bp of sequence found in GFP). A downstream fragment was amplified using primers FEM55GFPF2 (5′-ATGGACGAGCTG-TACAAGACAGAACAGACGAAGGCT-3′; contains 18 bp of sequence found in GFP) and FEM55R2 (5′-TTGAGTAACGCACTGAGCTTC-3′). The GFP insert was amplified from pBI-GFP(S65T) (Choi et al., 2002) using primers GFPfuseF1 (5′-ATGGTGAGCAAGGGCGAG-3′) and GFPfuseR1 (5′-CTTGT-ACAGCTCGTCCAT-3′). The GFP fragment contained the entire GFP open reading frame, excluding the stop codon. The three PCR fragments were gel purified using QIAquick spin columns and then used as the template for a PCR reaction using primers FEM55GFPF1 and FEM55R2, which resulted in a 1.8-kb fusion product containing a GFP and FEM55 sequence. This product was TOPO cloned and sequenced to verify that no PCR errors existed. The TOPO clone was then cut with *Acc*I and *Xho*I and inserted into NFD1-2.8/Topo at *Acc*I-*Xho*I to create NFD1-GFP/Topo. Finally, NFD1-GFP/Topo was cut with *Pst*I and was subcloned into pCAMBIA1300 at *Pst*I to create NFD1-GFP/pCambia.

Expression of GFP and MitoTracker stain was detected as described previously (Christensen et al., 2002), with the modification that roots were mounted in 1 × Murashige and Skoog salts.

RT-PCR

Tissue was harvested from plants and placed immediately into liquid nitrogen. Pistils were harvested from the oldest stage 12 flower (Smyth et al., 1990) on each plant. Floral cluster tissue includes the inflorescence meristem and flowers at stages 1 to 10 (Smyth et al., 1990). Silique tissue includes siliques at 1 to 2 d after pollination. Leaf tissue includes leaves of sizes 5 to 12 mm. Roots were harvested from seedlings at 11 d after germination. Floral stem tissue includes internodes from 4-week-old plants.

RNA was extracted from these tissues using the Qiagen RNeasy kit following the manufacturer's instructions (www.qiagen.com). DNA was removed from the RNAs using the Ambion TURBO DNA-free DNase kit following the manufacturer's instructions. Following DNase treatment, RNA samples were repurified using the Qiagen RNeasy kit following the manufacturer's instructions. Aliquots of RNA (1 μg) were reverse transcribed using the RETROscript kit (Ambion) following the manufacturer's instructions.

The PCR reaction mixture consisted of 0.5 μL of cDNA, 0.5 μM primers, 0.1 μL of Biolase DNA polymerase (E & K Scientific; www.eandkscientific.com), and 1 × standard PCR reaction mix. The PCR primers used to detect the *NFD1* transcript were RPL21M-RP (5′-TGCCGAGCCCAATAGAAGAAC-3′) and RPL21M-LB2 (5′-ACCGGCGGAGAAAGTGGAAGAG-3′). The PCR primers used to detect *ACTIN* transcripts were ACT.ConF (5′-GATTTGGCATCA-CACTTTCTACAATG-3′) and ACT.ConR (5′-GTTCCACCACTGAGCA-CAATG-3′). These primers are predicted to anneal to *ACTIN1* to *4*, *7*, *8*, *11*, and *12*. PCR was performed using a PTC-200 thermal cycler (MJ Research). The PCR program consisted of a first step of denaturation and polymerase activation (94°C for 2 min) followed by 30 cycles of denaturation for *NFD1* and 25 cycles of denaturation for *ACTIN* (94°C for 30 s), annealing (55°C for 5 s), and extension (68°C for 30 s).

Sequence Analysis

We used pfam 19.0 (http://pfam.wustl.edu/hmmsearch.shtml) to identify protein motifs. We used TargetP (http://www.cbs.dtu.dk/services/TargetP) to identify predicted protein localization signals/motifs. We used the Meg-Align module of the DNAStar Lasergene suite to align sequences; specifically, we used the Lipman-Pearson algorithm for the alignment of protein sequences and the Wilbur-Lipman algorithm for the alignment of the nucleotide sequences.

Linkage Analysis

For each mutant line, a plant hemizygous for the T-DNA insertion was crossed with wild-type pollen, and F_1 seed was collected and plated on germination medium containing 50 μg/mL kanamycin. One hundred kanamycin-resistant F_1 progeny were analyzed by PCR, using the primers described above, for the presence of the T-DNA insert that had been identified by TAIL-PCR. All plants that were kanamycin resistant contained the T-DNA insertion.

Image Processing

All images were processed for publication using Adobe Photoshop 7.0 and Adobe Illustrator 10.0 (Adobe Systems).

Accession Numbers

The gene structure and coding sequence of *NFD1* is based on two previously reported cDNAs (CERES:7876 and EMBL:BT005870.1; http://mips.gsf.de/cgi-bin/proj/thal/search_gene?code=at4g30925). The GenBank accession number for the NFD1 protein sequence is NP_567861.1. The Munich Information Center for Protein Sequences (MIPS) number for the protein sequence of NFD1 in this article is At4g30925. The Arabidopsis Genome Initiative (AGI) number for the protein sequence of NFD1 in this article is At4g30930. The GenBank accession number for the *E. coli* protein L21 is BAB37488.1.

ACKNOWLEDGMENTS

We thank members of the Drews lab for critical review of this manuscript.

Received February 15, 2006; revised April 28, 2006; accepted May 4, 2006; published May 12, 2006.

LITERATURE CITED

Alexander RW, Cooperman BS (1998) Ribosomal proteins neighboring 23 S rRNA nucleotides 803-811 within the 50 S subunit. Biochemistry **37:** 1714–1721

Beh CT, Brizzio V, Rose MD (1997) KAR5 encodes a novel pheromone-inducible protein required for homotypic nuclear fusion. J Cell Biol **139:** 1063–1076

Boisnard-Lorig C, Colon-Carmona A, Bauch M, Hodge S, Doerner P, Bancharel E, Dumas C, Haseloff J, Berger F (2001) Dynamic analyses of the expression of the HISTONE::YFP fusion protein in Arabidopsis show that syncytial endosperm is divided in mitotic domains. Plant Cell **13:** 495–509

Brizzio V, Khalfan W, Huddler D, Beh CT, Andersen SS, Latterich M, Rose MD (1999) Genetic interactions between KAR7/SEC71, KAR8/JEM1, KAR5, and KAR2 during nuclear fusion in Saccharomyces cerevisiae. Mol Biol Cell **10:** 609–626

Choi Y, Gehring M, Johnson L, Hannon M, Harada JJ, Goldberg RB, Jacobsen SE, Fischer RL (2002) DEMETER, a DNA glycosylase domain protein, is required for endosperm gene imprinting and seed viability in Arabidopsis. Cell **110:** 33–42

Christensen CA, Gorsich SW, Brown RH, Jones LG, Brown J, Shaw JM, Drews GN (2002) Mitochondrial GFA2 is required for synergid cell death in Arabidopsis. Plant Cell **14:** 2215–2232

Christensen CA, King EJ, Jordan JR, Drews GN (1997) Megagametogenesis in Arabidopsis wild type and the Gf mutant. Sex Plant Reprod **10:** 49–64

Christensen CA, Subramanian S, Drews GN (1998) Identification of gametophytic mutations affecting female gametophyte development in Arabidopsis. Dev Biol **202:** 136–151

Clough SJ, Bent AF (1998) Floral dip: a simplified method for Agrobacterium-mediated transformation of Arabidopsis thaliana. Plant J **16:** 735–743

Drews GN, Yadegari R (2002) Development and function of the angiosperm female gametophyte. Annu Rev Genet **36:** 99–124

Duzgunes N, Wilschut J, Fraley R, Papahadjopoulos D (1981) Studies on

the mechanism of membrane fusion. Role of head-group composition in calcium- and magnesium-induced fusion of mixed phospholipid vesicles. Biochim Biophys Acta **642:** 182–195

Emanuelsson O, Nielsen H, Brunak S, von Heijne G (2000) Predicting subcellular localization of proteins based on their N-terminal amino acid sequence. J Mol Biol **300:** 1005–1016

Faure JE, Mogensen HL, Dumas C, Lorz H, Kranz E (1993) Karyogamy after electrofusion of single egg and sperm cell protoplasts from maize: cytological evidence and time course. Plant Cell **5:** 747–755

Faure JE, Rotman N, Fortune P, Dumas C (2002) Fertilization in Arabidopsis thaliana wild type: developmental stages and time course. Plant J **30:** 481–488

Folsom MW, Peterson CM (1984) Ultrastructural aspects of the mature embryo sac of soybean, Glycine max (L.) Merr. Bot Gaz **145:** 1–10

Gavel Y, Nilsson L, von Heijne G (1988) Mitochondrial targeting sequences. Why 'non-amphiphilic' peptides may still be amphiphilic. FEBS Lett **235:** 173–177

Hancock LC, Behta RP, Lopes JM (2006) Genomic analysis of the Opiphenotype. Genetics doi/10.1534/genetics.106.057489

Huang B-Q, Russell SD (1992) Female germ unit: organization, isolation, and function. Int Rev Cytol **140:** 233–292

Jensen WA (1964) Observations on the fusion of nuclei in plants. J Cell Biol **23:** 669–672

Kasahara RD, Portereiko MF, Sandaklie-Nikolova L, Rabiger DS, Drews GN (2005) MYB98 is required for pollen tube guidance and synergid cell differentiation in Arabidopsis. Plant Cell **17:** 2981–2992

Lagrange T, Franzetti B, Axelos M, Mache R, Lerbs-Mache S (1993) Structure and expression of the nuclear gene coding for the chloroplast ribosomal protein L21: developmental regulation of a housekeeping gene by alternative promoters. Mol Cell Biol **13:** 2614–2622

Liu YG, Mitsukawa N, Oosumi T, Whittier RF (1995) Efficient isolation and mapping of Arabidopsis thaliana T-DNA insert junctions by thermal asymmetric interlaced PCR. Plant J **8:** 457–463

Maheshwari P, Johri BM (1950) Development of the embryo sac, embryo and endosperm in helixanthera ligustrina (wall.) dans. Nature **165:** 978–979

Maze J, Lin S-C (1975) A study of the mature megagametophyte of *Stipa elmeri*. Can J Bot **53:** 2958–2977

Ng DT, Walter P (1996) ER membrane protein complex required for nuclear fusion. J Cell Biol **132:** 499–509

Niewiadomski P, Knappe S, Geimer S, Fischer K, Schulz B, Unte US, Rosso MG, Ache P, Flugge UI, Schneider A (2005) The Arabidopsis plastidic glucose 6-phosphate/phosphate translocator GPT1 is essential for pollen maturation and embryo sac development. Plant Cell **17:** 760–775

Pagnussat GC, Yu HJ, Ngo QA, Rajani S, Mayalagu S, Johnson CS, Capron A, Xie LF, Ye D, Sundaresan V (2005) Genetic and molecular identification of genes required for female gametophyte development and function in Arabidopsis. Development **132:** 603–614

Philipp EI, Franke WW, Keenan TW, Stadler J, Jarasch ED (1976) Characterization of nuclear membranes and endoplasmic reticulum isolated from plant tissue. J Cell Biol **68:** 11–29

Roise D (1997) Recognition and binding of mitochondrial presequences during the import of proteins into mitochondria. J Bioenerg Biomembr **29:** 19–27

Rose MD (1996) Nuclear fusion in the yeast Saccharomyces cerevisiae. Annu Rev Cell Dev Biol **12:** 663–695

Samaha RR, Green R, Noller HF (1995) A base pair between tRNA and 23S rRNA in the peptidyl transferase centre of the ribosome. Nature **377:** 309–314

Santos-Rosa H, Leung J, Grimsey N, Peak-Chew S, Siniossoglou S (2005) The yeast lipin Smp2 couples phospholipid biosynthesis to nuclear membrane growth. EMBO J **24:** 1931–1941

Schulz P, Jensen WA (1973) *Capsella* embryogenesis: the central cell. J Cell Sci **12:** 741–763

Shimizu KK, Okada K (2000) Attractive and repulsive interactions between female and male gametophytes in Arabidopsis pollen tube guidance. Development **127:** 4511–4518

Smyth DR, Bowman JL, Meyerowitz EM (1990) Early flower development in Arabidopsis. Plant Cell **2:** 755–767

Sumner M, van Caeseele L (1990) The development of the central cell of *Brassica campestris* prior to fertilization. Can J Bot **68:** 2553–2563

Unseld M, Marienfeld JR, Brandt P, Brennicke A (1997) The mitochondrial genome of Arabidopsis thaliana contains 57 genes in 366,924 nucleotides. Nat Genet **15:** 57–61

van Went JL (1970) The ultrastructure of the fertilized embryo sac of Petunia. Acta Bot Neerl **19:** 468–480

van Went JL, Willemse MTM (1984) Fertilization. *In* B Johri, ed, Embryology of Angiosperms. Springer-Verlag, Berlin, pp 273–318

Vladimirov SN, Druzina Z, Wang R, Cooperman BS (2000) Identification of 50S components neighboring 23S rRNA nucleotides A2448 and U2604 within the peptidyl transferase center of Escherichia coli ribosomes. Biochemistry **39:** 183–193

Weterings K, Russell SD (2004) Experimental analysis of the fertilization process. Plant Cell (Suppl) **16:** S107–S118

Willemse MTM, van Went JL (1984) The female gametophyte. *In* BM Johri, ed, Embryology of Angiosperms. Springer-Verlag, Berlin, pp 159–196

Yadegari R, Drews GN (2004) Female gametophyte development. Plant Cell (Suppl) **16:** S133–S141